Mixed-state Hall scaling behavior and vortex phase diagram in $FeSe_{0.7}Te_{0.3}$ thin films

Dongwon Shin,[1,2] Soon-Gil Jung,[1,2,*] Sehun Seo,[3] Jongmin Lee,[3] Sanghan Lee,[3] Jin Hee Kim,[4] Jong-Soo Rhyee,[4] Woo Seok Choi,[2] and Tuson Park[1,2,†]

[1]*Center for Quantum Materials and Superconductivity (CQMS), Sungkyunkwan University, Suwon 16419, Republic of Korea*
[2]*Department of Physics, Sungkyunkwan University, Suwon 16419, Republic of Korea*
[3]*School of Materials Science and Engineering, Gwangju Institute of Science and Technology (GIST), Gwangju 61005, Republic of Korea*
[4]*Department of Applied Physics and Institute of Natural Sciences, Kyung Hee University, Yongin 17104, Republic of Korea*

(Received 8 December 2021; accepted 17 February 2022; published 28 February 2022)

We investigate the scaling behavior between Hall resistivity (ρ_{xy}) and longitudinal resistivity (ρ_{xx}) in the mixed state and the vortex phase diagram for $FeSe_{0.7}Te_{0.3}$ (FST) thin films. The ρ_{xy} and the ρ_{xx} are simultaneously measured as functions of temperature and magnetic field, and $\rho_{xy}(H, T)$ is expressed using the power law relation $\rho_{xy}(H, T) = A\rho_{xx}^{\beta}(H, T)$. Interestingly, FST thin films show a two-slope behavior in the power law relation with different exponent values of β_1 and β_2. For the temperature sweep (T sweep) at a fixed magnetic field, β_1 ($=2.0 \pm 0.16$) is insensitive to the magnetic field, whereas for the magnetic field sweep (H sweep) at a fixed temperature, the value significantly increases from 1.93 to 3.82 with an increase in temperature. On the other hand, changes in the β_2 value are relatively small for both cases. Two β_1 and β_2 values result in two vortex liquid regimes, which could be ascribed to different pinning strengths within the β_1 and β_2 regions. In addition, the tangent of the Hall angle ($\tan\theta_H$) with respect to the magnetic field exhibits a crossover behavior at the critical field H^*, which coincides with the magnetic field corresponding to the boundary of the β_1 and β_2 regimes. These results suggest that various β values are possible in FST thin films and are closely related to the flux pinning characteristics.

DOI: 10.1103/PhysRevB.105.064519

I. INTRODUCTION

Fe-based superconductors (FeSCs) have attracted significant attention in the study of their pairing mechanism and superconducting properties for practical applications because of their high superconducting transition temperature (T_c) and the strong field performance of the critical current density (J_c) [1–3]. In general, FeSCs can be classified into two groups: Fe-chalcogenides Fe*Ch* (*Ch* = Se, Te, and S) and Fe-pnictides Fe*Pn* (*Pn* = As and P) [4–8]. The Fe*Ch* system is suitable for investigating the intrinsic properties of FeSCs owing to its simple crystal structure compared with Fe*Pn* compounds, such as *Ln*OFeAs (*Ln* = rare earth elements, 1111 system) and AFe_2As_2 (*A* = alkaline earth elements, 122 system). In addition, the Fe*Ch* system has recently been intensively studied owing to the observation of electronic nematicity in FeSe [9] and potential Majorana bound states on the vortex core in $FeTe_{1-x}Se_x$ [10].

Vortex dynamics in type-II SCs is not only a fundamentally interesting phenomenon but also an extremely important area for practical applications because the motion of vortices generates power dissipation [11]. Hall scaling, the relationship between longitudinal (ρ_{xx}) and Hall (ρ_{xy}) resistivities in the mixed state of type-II SCs, is one of the representative methods for investigating vortex dynamics. In addition, an analysis of the Hall scaling behavior can provide the origin of the Hall effect related to vortex motion in type-II SCs. A quantized magnetic flux ($\phi_0 \approx 2.07 \times 10^{-15}\,\mathrm{T\,m^2}$), i.e., a vortex composed of a normal core, can penetrate into the type-II SC when $H_{c1} \leqslant H \leqslant H_{c2}$, and when an electric current is applied, vortices can be moved by the Lorentz force $\mathbf{F_L} = \mathbf{J} \times \mathbf{B}$, where H_{c1} and H_{c2} are the lower and upper critical fields, respectively, $\mathbf{J}$ is the applied current density, and $\mathbf{B}$ is the magnetic induction field corresponding to the product of the number of vortices and the magnitude of vortex ϕ_0. The Hall resistivity, i.e., ρ_{xy}, perpendicular to the $\mathbf{J}$ and $\mathbf{B}$ directions, is mainly generated by the motion of vortices produced by $\mathbf{F_L}$ [8,12].

The value of ρ_{xy} in the type-II SC mainly consists of two terms: quasiparticle scattering and vortex motion. Quasiparticle scattering is related to the motion of quasiparticles in the area of the vortex core, whereas vortex motion, which significantly contributes to the Hall effects, results in an electric field caused by the time-dependent magnetic flux. In addition, thermal fluctuations induce a thermally activated flux flow, which usually causes a broad SC transition, and the broadness becomes more noticeable with an increase in the magnetic field [13]. Consequently, the value of ρ_{xy} in the mixed state of type-II SCs is associated with longitudinal resistivity (ρ_{xx}) and can be expressed using the power law relation $\rho_{xy}(H, T) = A\rho_{xx}^{\beta}(H, T)$, where β is the scaling exponent, and A is almost constant [12].

Scaling exponent β values have been reported in both theoretical and experimental results [12,14–22]. Vinokur *et al.* [12] proposed a universal Hall scaling behavior with $\beta = 2$,

*prosgjung@gmail.com
†tp8701@skku.edu

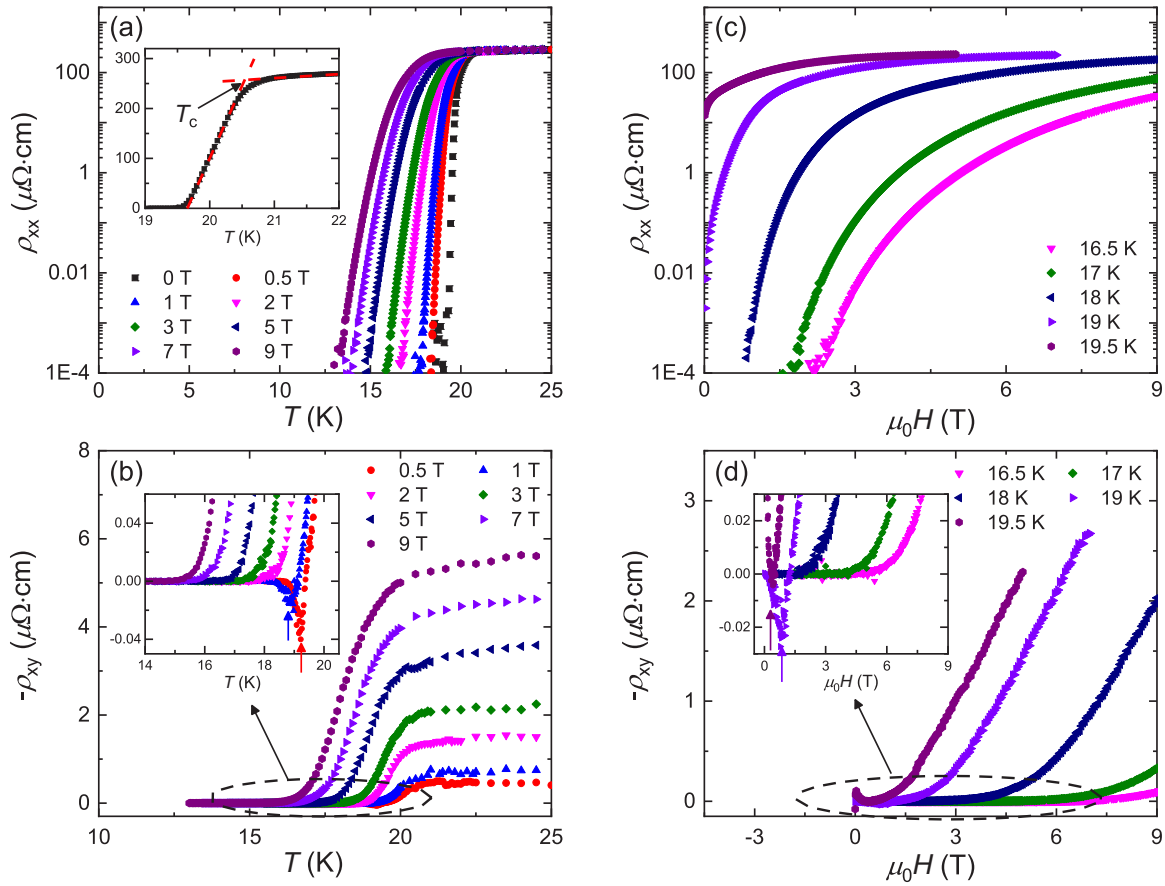

FIG. 1. Temperature dependence of (a) ρ_{xx} and (b) ρ_{xy} under a fixed magnetic field (T sweep) and magnetic field dependence of (c) ρ_{xx} and (d) ρ_{xy} at a fixed temperature (H sweep) for FST thin films. The inset in (a) represents the criterion of T_c used in this paper. The insets in (b) and (d) are magnified views of ρ_{xy}-T curves near zero resistivity for the T and H sweeps, respectively, showing the presence of a Hall sign anomaly near T_c and at low fields, as indicated by the arrows.

irrespective of the flux pinning strength. In contrast, Wang *et al.* [14] suggested changes in the β value from 2 to 1.5 when the flux pinning strength increases. These two models have been widely used to explain the experimental results for the Hall scaling behavior of type-II SCs such as high-T_c cuprates, MgB_2, and FeSCs [15–21]. However, experimental results with theoretically unexpected β values have been frequently reported [19,22–25]. For instance, a large β value of ~3–4 has been observed in Co-doped $BaFe_2As_2$ single crystals and K-doped $BaFe_2As_2$ thin films, which were thought to be due to weak pinning [22,24,26]. In contrast, a small value of $\beta \approx 1$, which is considered closely related to strong pinning, has been reported for Fe(Te,Se) single crystals and $HgBa_2CaCu_2O_{6+\delta}$ thin films with columnar defects [19,25]. Therefore, investigating vortex dynamics in correlation with the Hall scaling behavior is important to determine the origin of the β values beyond the theoretical approach.

In this paper, we investigated the Hall scaling behavior of thin films of $FeSe_{0.7}Te_{0.3}$ (FST) and its vortex phase diagram. The ρ_{xx} and ρ_{xy} for FST thin films were measured simultaneously in a temperature sweep (T sweep) at a fixed magnetic field and a magnetic field sweep (H sweep) at a fixed temperature. The value of ρ_{xy} of FST thin films in the power law relation $\rho_{xy} \propto \rho_{xx}^{\beta}$ was scaled with different exponents of β_1 and β_2 for both cases of the T and H sweeps, which led to two vortex liquid regimes of β_1 and β_2. The boundary between the β_1 and β_2 regions was found to be consistent with the critical field H^*, showing the crossover behavior in the field dependence of the tangent of the Hall angle ($\tan\theta_H$). Our results indicate that the Hall scaling relation in FST thin films is strongly influenced by the vortex motion associated with the flux pinning strength.

II. EXPERIMENTS

Highly c-axis-oriented FST thin films with a thickness of 100 nm were deposited on a CaF_2 (001) substrate with a size of 5 mm × 10 mm by using a pulsed laser deposition technique, and the details of the growth technique and the quality of the prepared thin films are described elsewhere [27]. The six-probe method was used to measure the longitudinal resistivity (ρ_{xx}) and the Hall resistivity (ρ_{xy}), which were simultaneously measured at the same magnetic field and temperature in a Physical Property Measurement System (PPMS 9 T, Quantum Design). Here, two measurement modes were used to obtain ρ_{xx} and ρ_{xy}, i.e., a magnetic field sweep (H sweep) at a fixed temperature and a temperature sweep (T sweep) in a fixed magnetic field. The direction of the

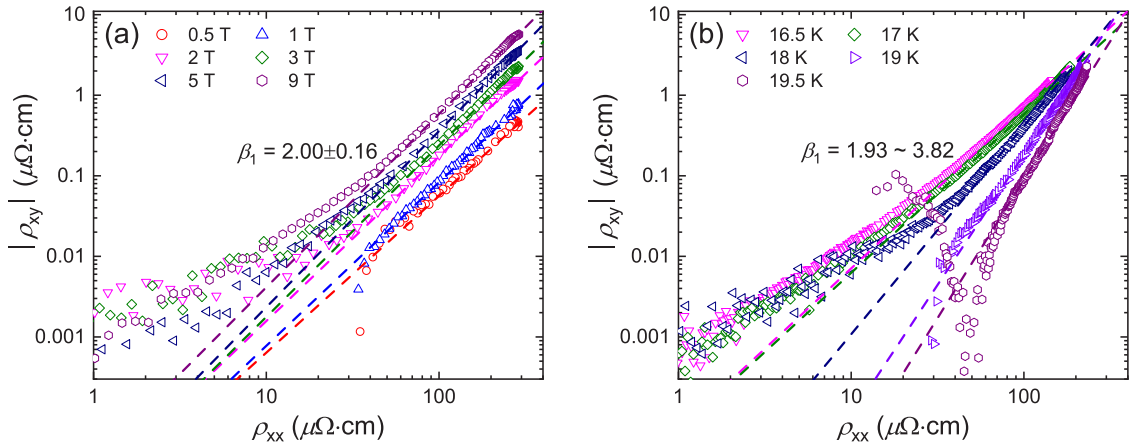

FIG. 2. Hall scaling behaviors of FST thin films for (a) the T sweep under various magnetic fields from 0.5 to 9 T and (b) the H sweep under various temperatures from 16.5 to 19.5 K. Dashed lines indicate the fitting results of the relation $\rho_{xy} \propto \rho_{xx}^{\beta}$, where β is the scaling factor that corresponds to the slope.

applied magnetic field was parallel to the c axis of the film and perpendicular to the applied electric current, and the size of the applied current density was ~400 A/cm^2. The value of ρ_{xy} was determined from the average value $\rho_{xy} = (\rho_{xy}^{+H} - \rho_{xy}^{-H})/2$, to eliminate the antisymmetric part of ρ_{xy}, where ρ_{xy}^{+H} and ρ_{xy}^{-H} indicate the Hall resistivities measured under a magnetic field applied parallel and antiparallel to the c axis of the film, respectively.

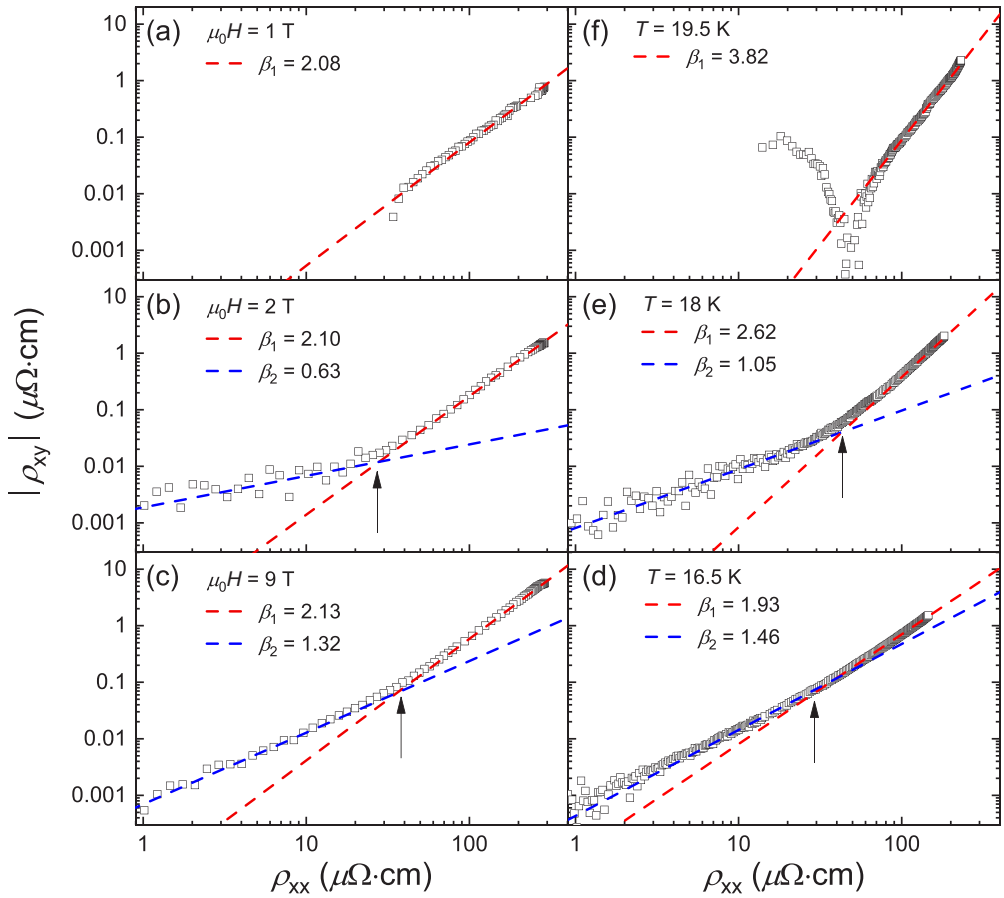

FIG. 3. Scaling behaviors between ρ_{xx} and ρ_{xy} of FST thin films for (a)–(c) the T sweep and (d)–(f) the H sweep at representative magnetic fields and temperatures, respectively. A two-slope behavior with different β values, β_1 and β_2, appeared at $\mu_0 H \geqslant 2$ T for the T sweep and at $T \leqslant 18$ K for the H sweep. Red and blue dashed lines indicate β_1 and β_2, respectively, and black arrows mark the crossover region between two different β values.

III. RESULTS AND DISCUSSION

Figures 1(a) and 1(b) show the temperature dependence of longitudinal resistivity (ρ_{xx}) and Hall resistivity (ρ_{xy}) for FST thin films under an external magnetic field of up to 9 T, respectively. The superconducting transition temperature (T_c) of the FST thin films is ~20.5 K, as presented in the inset of Fig. 1(a). Figures 1(c) and 1(d) show ρ_{xx} and ρ_{xy} as functions of the magnetic fields, respectively, at various fixed temperatures ranging from 16.5 to 19.5 K. The negative value of ρ_{xy} under a normal state indicates that the dominant charge carriers are electrons in FST thin films, whereas undoped FeSe thin films have a positive ρ_{xy} [28], which is thought to be related to a change in the electronic structure caused by the larger atomic radius of Te than that of Se [29,30]. Interestingly, FST thin films showed Hall sign anomaly at temperatures of around T_c and at low magnetic fields, as shown in the insets of Figs. 1(b) and 1(d), respectively. Similar behaviors have been observed in the FeSCs of Co-doped $BaFe_2As_2$ single crystals and $FeSe_{0.5}Te_{0.5}$ thin films and high-T_c cuprates, such as $YBa_2Cu_3O_{7-\delta}$ (YBCO) and $HgBa_2CaCu_2O_{6-\delta}$ [15,20,22,31]. Wang *et al.* [14] suggested that a sign reversal of ρ_{xy} in type-II SCs results from a pinning-induced backflow effect together with thermal fluctuations. However, the mechanism of the Hall sign anomaly in type-II SCs is still unclear owing to complicated vortex phenomena [32–34]. Further theoretical and detailed experimental studies are required to understand the mechanism of the Hall sign reversal in type-II SCs.

Figures 2(a) and 2(b) show the scaling behaviors between ρ_{xx} and ρ_{xy}, expressed by the power law relation $\rho_{xy} \propto \rho_{xx}^{\beta}$ of FST thin films for the T and H sweeps, respectively, where ρ_{xy} is indicated by the absolute value $|\rho_{xy}|$. For the T sweep at fixed magnetic fields of 0.5 to 9 T, ρ_{xy} was scaled with the exponent $\beta_1 = 2.0 \pm 0.16$, irrespective of the magnitude of the applied magnetic field, as shown in Fig. 2(a). In contrast, for the H sweep at fixed temperatures of 16.5 to 19.5 K, the value of β_1 increased gradually from 1.93 to 3.82 as the temperature increased, as shown in Fig. 2(b). The different β_1 values for the T and H sweeps suggest that the vortex dynamics in FST thin films are dependent on the type of sweep processes: T or H sweep.

Typically, type-II SCs have a single scaling exponent β value in the Hall scaling relation $\rho_{xy} \propto \rho_{xx}^{\beta}$ [15–20,22]; however, FST thin films show a two-slope behavior with different exponents of β_1 and β_2 for both T and H sweeps. Representative two-slope behaviors in the Hall scaling of FST thin films are shown in Fig. 3. For the T sweep, ρ_{xy} was well scaled with a single exponent β_1 of up to 1 T; however, another scaling region appeared at $\mu_0 H \geqslant 2$ T, as shown in Figs. 3(a)–3(c). The H sweep also showed a two-slope behavior for $T \leqslant 18$ K, as shown in Figs. 3(d)–3(f), where the crossover points are indicated by the arrows.

The scaling exponents β_1 and β_2 with respect to the magnetic field and temperature for the T and H sweeps are summarized in Figs. 4(a) and 4(b), respectively. The exponent β_1 for the T sweep was ~2, which is almost independent of the magnetic field, whereas that for the H sweep showed a large increase from 1.93 to 3.82 with increasing temperature. The β_2 values for the T and H sweeps barely changed after

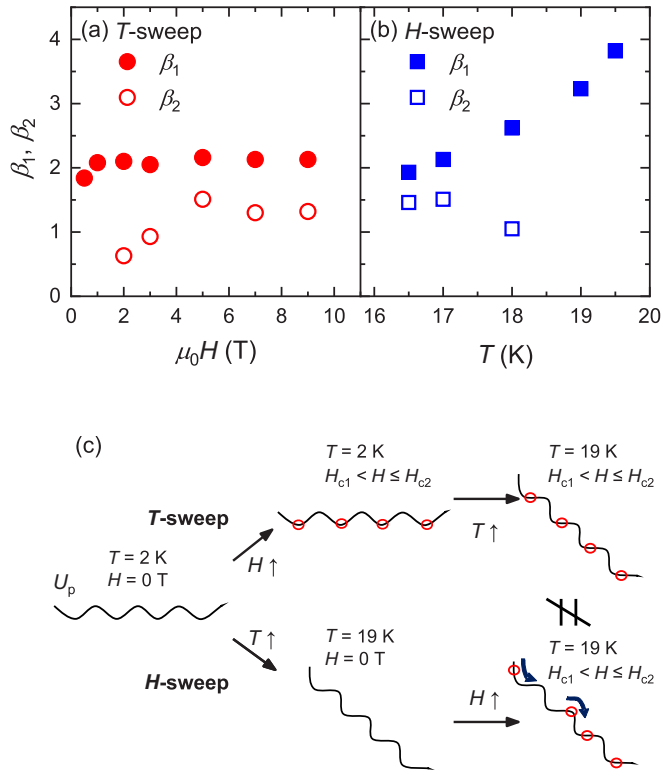

FIG. 4. The β_1 and β_2 values of FST thin films for (a) the T sweep and (b) the H sweep under various magnetic fields and temperatures, respectively. The value of β_1 is almost independent of magnetic field in the T-sweep mode, whereas it gradually increases with temperature in the H-sweep mode. (c) Simple diagram for different flux flow processes between T and H sweeps, where U_p is the effective pinning potential, and the red circle indicates a vortex. For the T sweep under a fixed magnetic field, penetrated vortices can be stably trapped on the pinning centers. By contrast, for an H sweep at a fixed temperature, the relationship between the magnitude of U_p and the thermal activation energy play an important role. For instance, the vortices introduced may not be effectively pinned to the pinning sites because the effect of thermal fluctuations is relatively large at temperatures near T_c, thus promoting a vortex motion and large β values.

an initial decrease under low magnetic fields and high temperatures, respectively. The Hall scaling behavior with $\beta \approx 2$ for the T sweep agreed with the phenomenological model proposed by Vinokur *et al.* [12]. They suggested the universal scaling law $\rho_{xy} \propto \rho_{xx}^2$ irrespective of the type of pinning sites and vortex states, such as a vortex glass, vortex liquid, thermally activated flux flow, and flux flow [12].

However, a large increase in β values exhibited in the H sweep has not been predicted in any model thus far. Wang, Dong, and Ting (WDT) developed another model that considers both thermal fluctuations and flux pinning and showed that β values varied from 2 to 1.5, with an increase in the pinning strength [14]. Based on the WDT model, a noticeable increase in β_1 values in the H sweep for FST thin films can be closely associated with the change in pinning strength from strong to weak pinning with an increase in temperature [14]. Because the thermal effect on the vortices becomes significant as the temperature approaches T_c, the effective pinning

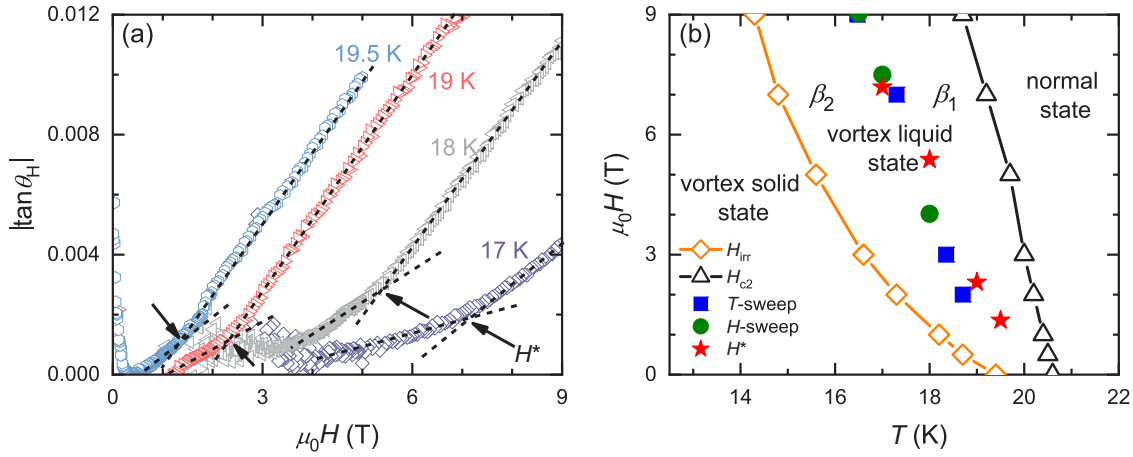

FIG. 5. (a) Magnetic field dependence of the absolute value of $\tan\theta_H$, $|\tan\theta_H|$, in FST thin film for several fixed temperatures. There are two linear parts, and the crossover field between them ($= H^*$) is indicated by the arrows. The dashed lines are guides to the eyes. (b) The vortex phase diagram of FST thin films shows two vortex liquid regions divided by different β values of β_1 and β_2, and the boundary of two vortex liquid regions are consistent with H^*.

potential (U_p) can be relatively small, which can lead to a large exponent β [22,35]. Similar results for the large β values were observed in $YBa_2Cu_3O_y/PrBa_2Cu_3O_y$ superlattices, Co-doped $BaFe_2As_2$ single crystals, and K-doped $BaFe_2As_2$ thin films, and a weak flux pinning was suggested as a reason for the large exponent $\beta > 2$ [22,24,26,35].

To understand the changes in the β_1 value in the H sweep, a simple diagram of the vortex-pin interactions in the cases of T and H sweeps for FST thin films is shown in Fig. 4(c). For the T sweep, the vortices can initially penetrate into type-II SCs when the applied magnetic field is larger than the low critical field (H_{c1}); in addition, at a certain magnetic field and at 0 K, most of the introduced vortices can be trapped in the pinning sites, if the number of pinning sites is similar to the number of vortices, and the pinned vortices will then begin to creep or move gradually as the temperature increases because the thermal effect reduces U_p. In contrast, for the H sweep, the number of vortices gradually increases with an increase in the magnetic field, and the introduced vortices are relatively difficult to be immediately captured in weak pinning sites than in strong pinning sites. Therefore, particularly at high temperatures close to T_c, the introduced vortices can be easily mobile. These scenarios indicate that the flux pinning effect on the H sweep can effectively weaken with an increase in temperature, resulting in the possibility of an increase in β as the temperature approaches T_c [36].

Figure 5(a) shows the magnetic field dependence of the tangent of the Hall angle ($|\tan\theta_H|$) for FST thin films. Here, $|\tan\theta_H|$ given by ρ_{xy}/ρ_{xx} was expressed as an absolute value owing to the negative value of ρ_{xy}, as presented in Fig. 1(b). The value of $|\tan\theta_H|$ with respect to the magnetic field exhibited two linear parts within the temperature range of 17 to 19.5 K, and the crossover point (H^*) is indicated by the arrows. Since the Hall angle is strongly related to the vortex motion, different slopes of the field dependence of $|\tan\theta_H|$ at the boundary H^* indicate the existence of different vortex dynamics, which can be attributed to the different vortex liquid regimes [37,38].

Figure 5(b) shows the T-H vortex phase diagram of the FST thin films. Based on the results of Hall scaling and $|\tan\theta_H|$, the vortex states of FST thin films were divided into three regions: a vortex solid region and two vortex liquid regions. Here, the vortex solid state was determined within the irreversible field (H_{irr} at $\rho_{xx} \to 0$), and the vortex liquid state was separated into β_1 and β_2 regimes, as shown in Figs. 2 and 3. Interestingly, the value of H^* defined at the crossover point of $|\tan\theta_H|$ against the magnetic field is close to the magnetic field corresponding to the boundary of the β_1 and β_2 regimes, indicating that the origin of the crossover behavior in $|\tan\theta_H|$ is like the two-slope behavior in the Hall scaling behavior $\rho_{xy} \propto \rho_{xx}^{\beta}$. These discoveries evidence that the two scaling exponents of β_1 and β_2 and the large change in β_1 in the H sweep are associated with the flux pinning characteristics of FST thin films, such as the number of effective pinning sites and changes in the effective pinning potential against temperature.

IV. CONCLUSIONS

In summary, we studied the scaling behavior between ρ_{xx} and ρ_{xy} for FST thin films and their vortex phase diagram. The FST thin films followed the power law relation $\rho_{xy} \propto \rho_{xx}^{\beta}$, where two exponents of β_1 and β_2 are observed for both T and H sweeps. The scaling exponent β_1 for the T sweep was ~2, which was independent of the magnetic field. In contrast, for the H sweep, the β_1 value significantly increased from 1.93 to 3.82 as T increased. Changes in β_2 for both sweep processes were insignificant when compared with the changes in β_1. The vortex liquid state in the vortex phase diagram of FST thin films was divided into two regions, which were signified by the different exponents of β_1 and β_2. The boundary of the two vortex liquid regions corresponded to the critical field H^* at which the crossover behavior appeared in the field dependence of the tangent of the Hall angle. These results underline that a wide range of β values of FST thin films in the Hall scaling relation $\rho_{xy} \propto \rho_{xx}^{\beta}$ is strongly influenced by the vortex motion

associated with the effective pinning potential related to the thermal activation energy.

ACKNOWLEDGMENTS

This study was supported by the National Research Foundation (NRF) of Korea through a grant funded by the Korean Ministry of Science and ICT (No. 2021R1A2C2010925 and No. 2021R1A2C2011340) and by the Basic Science Research Program through the NRF of Korea funded by the Ministry of Education (NRF-2021R1I1A1A01043885). This research was also supported by Creative Materials Discovery Program (No. 2017M3D1A1040834) through the NRF funded by the Ministry of Science and ICT.

[1] Y. Kamihara, T. Watanabe, M. Hirano, and H. Hosono, Iron-based layered superconductor $La[O_{1-x}F_x]FeAs$ ($x = 0.05$–0.12) with $T_c = 26$ K, J. Am. Chem. Soc. **130**, 3296 (2008).

[2] E. Pomjakushina, K. Conder, V. Pomjakushin, M. Bendele, and R. Khasanov, Synthesis, crystal structure, and chemical stability of the superconductor $FeSe_{1-x}$, Phys. Rev. B **80**, 024517 (2009).

[3] B. D. Josephson, Potential differences in the mixed state of superconductors, Phys. Lett. **16**, 242 (1965).

[4] F.-C. Hsu, J.-Y. Luo, K.-W. Yeh, T.-K. Chen, T.-W. Huang, P. M. Wu, Y.-C. Lee, Y.-L. Huang, Y.-Y. Chu, D.-C. Yan, and M.-K. Wu, Superconductivity in the PbO-type structure α-FeSe, Proc. Natl. Acad. Sci. USA **105**, 14262 (2008).

[5] J. H. Tapp, Z. Tang, B. Lv, K. Sasmal, B. Lorenz, P. C. W. Chu, and A. M. Guloy, LiFeAs: An intrinsic FeAs-based superconductor with $T_c = 18$ K, Phys. Rev. B **78**, 060505(R) (2008).

[6] M. Rotter, M. Tegel, and D. Johrendt, Superconductivity at 38 K in the Iron Arsenide $(Ba_{1-x}K_x)Fe_2As_2$, Phys. Rev. Lett. **101**, 107006 (2008).

[7] X. Zhu, F. Han, G. Mu, B. Zeng, P. Cheng, B. Shen, and H. -H. Wen, $Sr_3Sc_2Fe_2As_2O_5$ as a possible parent compound for FeAs-based superconductors, Phys. Rev. B **79**, 024516 (2009).

[8] H. Ogino, K. Machida, A. Yamamoto, K. Kishio, J. -i. Shimoyama, T. Tohei, and Y. Ikuhara, A new homologous series of iron pnictide oxide superconductors $(Fe_2As_2)(Ca_{n+2}(Al, Ti)_nO_y)$ ($n = 2, 3, 4$), Supercond. Sci. Technol. **23**, 115005 (2010).

[9] A. Fedorov, A. Yaresko, T. K. Kim, Y. Kushnirenko, E. Haubold, T. Wolf, M. Hoesch, A. Grüneis, B. Büchner, and S. V. Borisenko, Effect of nematic ordering on electronic structure of FeSe, Sci. Rep. **6**, 36834 (2016).

[10] D. Wang, L. Kong, P. Fan, H. Chen, S. Zhu, W. Liu, L. Cao, Y. Sun, S. Du, J. Schneeloch, R. Zhong, G. Gu, L. Fu, H. Ding, and H.-J. Gao, Evidence for Majorana bound states in an iron-based superconductor, Science **362**, 333 (2018).

[11] M. Checchin and A. Grassellino, Vortex Dynamics and Dissipation under High-Amplitude Microwave Drive, Phys. Rev. Appl. **14**, 044018 (2020).

[12] V. M. Vinokur, V. B. Geshkenbein, M. V. Feigel'man, and G. Blatter, Scaling of the Hall Resistivity in High-T_c Superconductors, Phys. Rev. Lett. **71**, 1242 (1993).

[13] D. Ahmad, W. J. Choi, Y. I. Seo, S. Seo, S. Lee, and Y. S. Kwon, Thermally activated flux flow in superconducting epitaxial $FeSe_{0.6}Te_{0.4}$ thin film, Results Phys. **7**, 16 (2017).

[14] Z. D. Wang, J. Dong, and C. S. Ting, Unified Theory of Mixed State Hall Effect in Type-II Superconductors: Scaling Behavior and Sign Reversal, Phys. Rev. Lett. **72**, 3875 (1994).

[15] J. Luo, T. P. Orlando, J. M. Graybeal, X. D. Wu, and R. Muenchausen, Scaling of the Longitudinal and Hall Resistivities from Vortex Motion in YBa_2Cu_3O, Phys. Rev. Lett. **68**, 690 (1992).

[16] R. C. Budhani, S. H. Liou, and Z. X. Cai, Diminishing Sign Anomaly and Scaling Behavior of the Mixed-State Hall Resistivity in $Tl_2Ba_2Ca_2Cu_3O_{10}$ Films Containing Columnar Defects, Phys. Rev. Lett. **71**, 621 (1993).

[17] A. V. Samoilov, Universal Behavior of the Hall Resistivity of Single Crystalline $Bi_2Sr_2CaCuO_x$ in the Thermally Activated Flux Flow Regime, Phys. Rev. Lett. **71**, 617 (1993).

[18] W. N. Kang, D. H. Kim, S. Y. Shim, J. H. Park, T. S. Hahn, S. S. Choi, W. C. Lee, J. D. Hettinger, K. E. Gray, and B. Glagola, Pinning Strength Dependence of Mixed-State Hall Effect in YBa_2Cu_3O Crystals with Columnar Defects, Phys. Rev. Lett. **76**, 2993 (1996).

[19] W. N. Kang, B. W. Kang, Q. Y. Chen, J. Z. Wu, S. H. Yun, A. Gapud, J. Z. Qu, W. K. Chu, D. K. Christen, R. Kerchner, and C. W. Ch, Scaling of the Hall resistivity in epitaxial $HgBa_2CaCu_2O_{6+\delta}$ thin films with columnar defects, Phys. Rev. B **59**, R9031(R) (1999).

[20] W. N. Kang, S. H. Yun, and J. Z. Wu, Scaling behavior and mixed-state Hall effect in epitaxial $HgBa_2CaCu_2O_{6+\delta}$ thin films, Phys. Rev. B **55**, 621 (1997).

[21] W. N. Kang, H.-J. Kim, E.-M. Choi, H. J. Kim, K. H. P. Kim, and S.-I. Lee, Universal scaling of the Hall resistivity in MgB_2 superconductors, Phys. Rev. B **65**, 184520 (2002).

[22] L. M. Wang, U.-C. Sou, H. C. Yang, L. J. Chang, C.-M. Cheng, K.-D. Tsuei, Y. Su, T. Wolf, and P. Adelmann, Mixed-state Hall effect and flux pinning in $Ba(Fe_{1-x}Co_x)_2As_2$ single crystals ($x = 0.08$ and 0.10), Phys. Rev. B **83**, 134506 (2011).

[23] C. Reichhardt, C. J. Olson, and F. Nori, Dynamic Phases of Vortices in Superconductors with Periodic Pinning, Phys. Rev. Lett. **78**, 2648 (1997).

[24] E. Son, N. H. Lee, T.-J. Hwang, D. H. Kim, and W. N. Kang, Hall effect of K-doped $BaFe_2As_2$ superconducting thin films, Prog. Supercond. Cryog. **15**, 5 (2013).

[25] H. Lei, R. Hu, E. S. Choi, and C. Petrovic, Thermally activated energy and flux-flow Hall effect of $Fe_{1+y}(Te_{1+x}S_x)_z$, Phys. Rev. B **82**, 134525 (2010).

[26] L. M. Wang, H. C. Yang, and H. E. Horng, Mixed-State Hall Effect in $YBa_2Cu_3O_y/PrBa_2Cu_3O_y$ Superlattices, Phys. Rev. Lett. **78**, 527 (1997).

[27] S. Seo, J.-H. Kang, M. J. Oh, I.-S. Jeong, J. Jiang, G. Gu, J.-W. Lee, J. Lee, H. Noh, M. Liu, P. Gao, E. E. Hellstrom, J.-H. Lee, Y. J. Jo, C.-B. Eom, and S. Lee, Origin of the emergence of higher T_c than bulk in iron chalcogenide thin films, Sci. Rep. **7**, 9994 (2017).

[28] M. Kawai, F. Nabeshima, and A. Maeda, Transport properties of FeSe epitaxial thin films under in-plane strain, J. Phys. Conf. Ser. **1054**, 012023 (2018).

[29] F. Sun, Z. Guo, H. Zhang, and W. Yuan, S/Te co-doping in tetragonal FeSe with unchanged lattice parameters: Effects on superconductivity and electronic structure, J. Alloys Compd. **700**, 43 (2017).

[30] J. Zhuang, W. K. Yeoh, X. Cui, X. Xu, Y. Du, Z. Shi, S. P. Ringer, X. Wang, and S. X. Dou, Unabridged phase diagram for single-phased $FeSe_xTe_{1-x}$ thin films, Sci. Rep. **4**, 7273 (2014).

[31] R. Ogawa, T. Ishikawa, M. Kawai, F. Nabeshima, and A. Maeda, Direct current measurement of Hall effect in the mixed state for the iron-chalcogenide superconductors, J. Phys. Conf. Ser. **1054**, 012021 (2018).

[32] M. Galffy and E. Zirngiebl, Hall-effect of bulk $YBa_2Cu_3O_{7-\delta}$, Solid State Commun. **68**, 929 (1988).

[33] S. J. Hagen, C. J. Lobb, R. L. Greene, M. G. Forrester, and J. H. Kang, Anomalous Hall effect in superconductors near their critical temperatures, Phys. Rev. B **41**, 11630 (1990).

[34] Y. Iye, S. Nakamura, and T. Tamegai, Hall effect in high temperature superconductors near T_c, Physica C **159**, 616 (1989).

[35] N. Haberkorn, M. Xu, W. R. Meier, J. Schmidt, S. L. Bud'ko, and P. C. Canfield, Effect of Ni doping on vortex pinning in $CaK(Fe_{1-x}Ni_x)_4As_4$ single crystals, Phys. Rev. B **100**, 064524 (2019).

[36] H. Sato, T. Katase, W. N. Kang, H. Hiramatsu, T. Kamiya, and H. Hosono, Anomalous scaling behavior in a mixed-state Hall effect of a cobalt-doped $BaFe_2As_2$ epitaxial film with a high critical current density over $1\,MA/cm^2$, Phys. Rev. B **87**, 064504 (2013).

[37] W.-S. Kim, W. N. Kang, M.-S. Kim, and S.-I. Lee, Vortex phase diagram of $HgBa_2Ca_2Cu_3O_{8+\delta}$ thin films from magnetoresistance measurements, Phys. Rev. B **61**, 11317 (2000).

[38] S.-G. Jung, W. K. Seong, J. Y. Huh, T. G. Lee, W. N. Kang, E.-M. Choi, H.-J. Kim, and S.-I. Lee, Hall conductivity and the vortex phase in MgB_2 thin films, Supercond. Sci. Technol. **20**, 129 (2007).